

# Computational Analysis of Flow in A De Laval Nozzle

Suvan Rao

*Received August 27, 2024*

*Accepted September 17, 2024*

*Electronic access November 30, 2024*

A nozzle is a device designed to modify or direct the flow of a fluid. It is mostly used to increase the velocity of fluid, subsequently generating thrust. A typical De-Laval nozzle is a nozzle which has a converging part, throat and diverging part. This paper aims to explain the effect of throat diameter on the thrust and gas exit velocity in a propulsion nozzle or the De Laval nozzle. Computational analysis of flow is done for different throat diameters. Using computational fluid dynamics, variation in different flow properties such as speed, pressure, temperature and density are visualized. Variations in thrust and drag force on the nozzle are also analyzed and compared.

## Introduction

The De Laval nozzle, also known as a convergent-divergent nozzle, is a critical component in various propulsion systems, including rockets and jet engines. Its unique design allows for the acceleration of gases to supersonic speeds, making it indispensable in both aerospace and industrial applications. The throat diameter, the narrowest part of the nozzle, plays a pivotal role in determining the overall performance of the nozzle. This research paper aims to investigate the impact of the throat diameter on two key performance metrics: thrust and gas exit velocity. Understanding the relationship between the throat diameter and these performance metrics is essential for optimizing nozzle design. Thrust, the force generated by the nozzle, directly influences the efficiency and power of propulsion systems. Gas exit velocity, on the other hand, is crucial for achieving the desired supersonic speeds and ensuring effective propulsion.

Several studies have investigated the flow behavior within such nozzles and the main findings are briefly summarized here. Previous studies on flow dynamics within such nozzles have been conducted by Patel et al. (2016), Deshpande and Vidwans (2014), and Gautam (2024).

Specifically Patel<sup>1</sup> et al. simulated flow through a CD nozzle using Ansys Fluent to study shockwaves, finding good agreement with analytical theory. This paper explains all the basic concepts of De Laval nozzle along with providing a simulation for each case.

Deshpande<sup>2</sup> et al. conducted a similar study, analyzing shock-wave evolution along the nozzle. Velocity, temperature and pressure have been calculated theoretically at different cross-sections of the nozzle using the formulated equations in this paper followed by verifying the theoretical results with the help of a computer simulation approach.

Gautam<sup>3</sup> simulated flow through a de Laval nozzle using incompressible Navier-Stokes equations for an inviscid fluid,

showing excellent agreement with 1D isentropic flow predictions.

Osman<sup>4</sup> et al. conducted a similar study to Gautam, confirming CFD results align well with 1D isentropic flow models. Results in their figures demonstrate good agreement with these studies' findings. The above studies represent a large body of work that has been conducted to study fluid behavior within nozzles. However, systematic studies regarding the explicit effect of the nozzle throat diameter would be useful to understand its effect, and ultimately optimize nozzle design.

By examining how variations in the throat diameter affect these parameters, this study seeks to provide insights that could enhance the design and functionality of De Laval nozzles. In this paper, we will explore a detailed analysis of how changes in the throat diameter influence thrust and gas exit velocity. To achieve this, we use the Euler equations to simulate inviscid, adiabatic flow through a De Laval nozzle. It is appropriate to use inviscid flow simulation at high flow rate or at a high Reynold's number. Subsequently, the resulting pressure and velocity fields are used to compute the thrust acting on the nozzle. These findings aim to contribute to the body of knowledge in nozzle design and propulsion technology, offering practical implications for improving the efficiency and performance of propulsion systems.

## Methodology

### Flowsquare

Flowsquare is a two-dimensional computational fluid dynamics (CFD) software designed for simulating unsteady flows. It allows users to model both non-reactive and reactive flows, including premixed and non-premixed mixtures, as well as subsonic and supersonic flows. Note that subsonic flow is the type of flow where the fluid speed remains below the speed of sound.

Supersonic flow is the type of flow that exceeds the speed of sound.

### Simulation Parameters

Simulation Parameters used for the analysis are as follows, The simulation is set to Euler mode, which is ideal for inviscid flow simulations where viscosity is negligible. This mode focuses on capturing large-scale flow features without the computational expense of resolving viscous effects. The grid resolution is 448 pixels in the x-direction and 224 pixels in the y-direction, determining the smallest scales of motion that can be resolved. Higher resolutions can capture finer details but require more computational resources. The domain size is 0.60 units in the x-direction and 0.30 units in the y-direction, with an aspect ratio of 2:1, indicating a rectangular domain suited for flows with significant variations in one direction.

No periodic boundary conditions are applied, suggesting that the boundaries are either reflective or open, influencing how waves and other flow features interact with the domain boundaries. The pressure is set at 1.0E+05 Pa, representing standard atmospheric pressure, a common assumption for simulations at sea level under normal conditions. The initial velocity is set to 300.0 units, defining the initial momentum and fluid flow evolution. The simulation employs a 4th-order Lax-Wendroff numerical scheme (iorder = 3; iorder is a finite order scheme used to solve the equations of fluid dynamics) to enhance accuracy by reducing numerical dissipation and dispersion errors. Filtering parameters (nfil = 1, wfil = 0.02; nfil refers to the number of filtering steps during each simulation and wfil controls the strength of the filter) are also utilized to manage numerical stability and accuracy. Note that the simulations here are coarse grained and filtered in Flowsquare and as a result do not explicitly capture turbulence.

We simulated the flow of a fluid through the geometry of a De Laval Nozzle in Flowsquare and analyzed the coherent variations in parameters across different throat diameters.

At the location where the nozzle area is the smallest, the Mach number reaches to 1 and the fluid moves at a sonic speed. After that, the velocity continues to increase due to gas expansion to reach supersonic speed near the exit. The exit fluid speed can be obtained theoretically using the following equation.

$$v_e = \sqrt{\frac{TR}{M} \cdot \frac{2\gamma}{\gamma-1} \cdot \left[ 1 - \left( \frac{p_e}{p} \right)^{\frac{\gamma-1}{\gamma}} \right]} \quad (1)$$

where

$v_e$  = exit velocity (m/s)

$T$  = inlet temperature (K)

$R$  = Universal gas constant (8314J/(kmol·K))

$p$  = absolute inlet pressure (Pa)

$\gamma$  = isentropic expansion factor (= 1.4 in flowsquare)

$p_e$  = absolute exhaust pressure (Pa)

$M$  = gas molar weight (g/mol)

### Euler's Equation

The Euler's Equations are a set of partial differential equations governing adiabatic flow assuming zero viscosity and zero thermal conductivity.

The equations are given by,

$$\frac{Dp}{Dt} = -\rho \nabla \cdot \mathbf{u} \quad (2)$$

$$\frac{D\mathbf{u}}{Dt} = -\frac{\nabla p}{\rho} + \mathbf{g} \quad (3)$$

$$\frac{De}{Dt} = -\frac{p}{\rho} \nabla \cdot \mathbf{u} \quad (4)$$

where,

Where,  $\mathbf{u}$  is the flow velocity vector,  $\rho$  is the fluid mass density,  $p$  is the pressure of the fluid, where  $p = \rho w$ ,  $e$  is the internal energy of the fluid,  $\mathbf{g}$  represents body accelerations such as gravity, internal acceleration, and acceleration due to the electric field, and  $D$  is the derivative with respect to time.

The equations above represent conservation of mass, momentum and energy. While the energy equation is expressed in terms of internal energy to illustrate its connection to the case of incompressible fluids, it is not in its simplest form.

### Nozzle Parameters and Geometry

The nozzle used for simulation was of length 60 centimeters in the horizontal direction and 30 centimeters in the vertical direction. A resolution of 448 pixels along the x-axis and 224 pixels along the y-axis was used for the simulation environment.

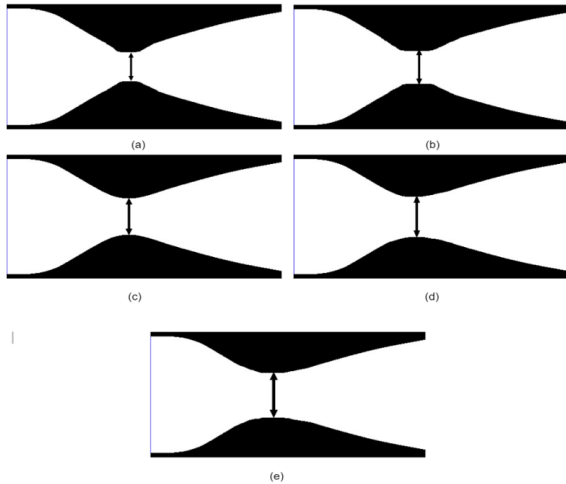
The throat diameter of the base nozzle is modified by increasing and decreasing through 2 steps of 7 units respectively. Minor geometric errors during modification have been neglected due to infinitesimally small values.

Figure 1 shows the geometry of the nozzle being analyzed. The throat of the base nozzle has been expanded and contracted to 7 and 14 pixels respectively.

The base nozzle (c) has a throat diameter of 66 pixels ~ 88.39 mm. This has been increased and decreased symmetrically by 7 and 14 pixels as seen in figures (a) and (b), and (d) and (e) respectively.

### Calculation of Drag and Lift

Calculation of lift and drag was done using a code programmed in C. This code reads velocity and pressure data from binary files, then uses this data to calculate drag and lift forces. It does



**Fig. 1** Nozzle geometries; (a) 14 pixels contracted; (b) 7 pixels contracted; (c) base nozzle; (d) 7 pixels expanded; (e) 14 units expanded

so by integrating pressure differences across the boundaries where the flow velocity is zero (indicating a surface, such as an object in the flow).

#### Lift calculation

For each column ( $i$ ) of the grid, the code integrates the pressure difference from the top and bottom edges where the velocity is zero, representing the lift force.

#### Drag calculation

For each row ( $j$ ) of the grid, the code integrates the pressure difference from the left and right edges where the velocity is zero, representing the drag force. It has the following theoretical implications,

1. **Grid and Domain Configuration:** The simulation is performed on a grid with dimensions of 448 by 224 points, corresponding to a physical domain size of 0.6 units in the x-direction and 0.3 units in the y-direction. This configuration suggests a focus on capturing fine-scale flow features within a relatively small domain, allowing for detailed analysis of flow behavior around objects or boundaries.
2. **Boundary Detection and Force Calculation:** The code identifies regions where the velocity is zero, effectively locating the boundaries of an object within the flow field. By integrating the pressure differences at these boundary points, the code calculates the drag and lift forces acting on the object. This method directly correlates pressure variations across the object's surface with the aerodynamic forces experienced, providing a quantitative measure of the object's interaction with the fluid.
3. **Pressure-Driven Force Dynamics:** The lift force is computed by summing the pressure differences between the

top and bottom of the object, reflecting how pressure imbalances in the vertical direction generate lift. Similarly, drag is calculated from the pressure differences along the horizontal edges, indicating how the fluid's resistance to the object's motion is quantified. These calculations are fundamental in understanding the aerodynamic efficiency and stability of objects within a flow, such as airfoils or vehicles.

#### 4. Efficiency in Computational Fluid Dynamics (CFD):

The code's use of binary file inputs and streamlined looping structures demonstrates an efficient approach to handling large datasets typical in CFD simulations. By minimizing file, I/O operations and focusing on in-memory computations, the code is optimized for performance, allowing it to handle high-resolution grids and complex flow fields with reduced computational overhead.

Out of the two components-shear and normal force-only the normal forces due to pressure can be calculated as viscosity is assumed to be zero.

## Results

Figure 2 shows the fluid speed (velocity magnitude) for the flow through each of the five nozzles. Note that the simulation was run to a time of 8.0 ms (the flow was observed to be steady at this time). From Figure 2, it can see that the nozzles with a smaller throat diameter have a higher maximum fluid speed (in the diverging section).

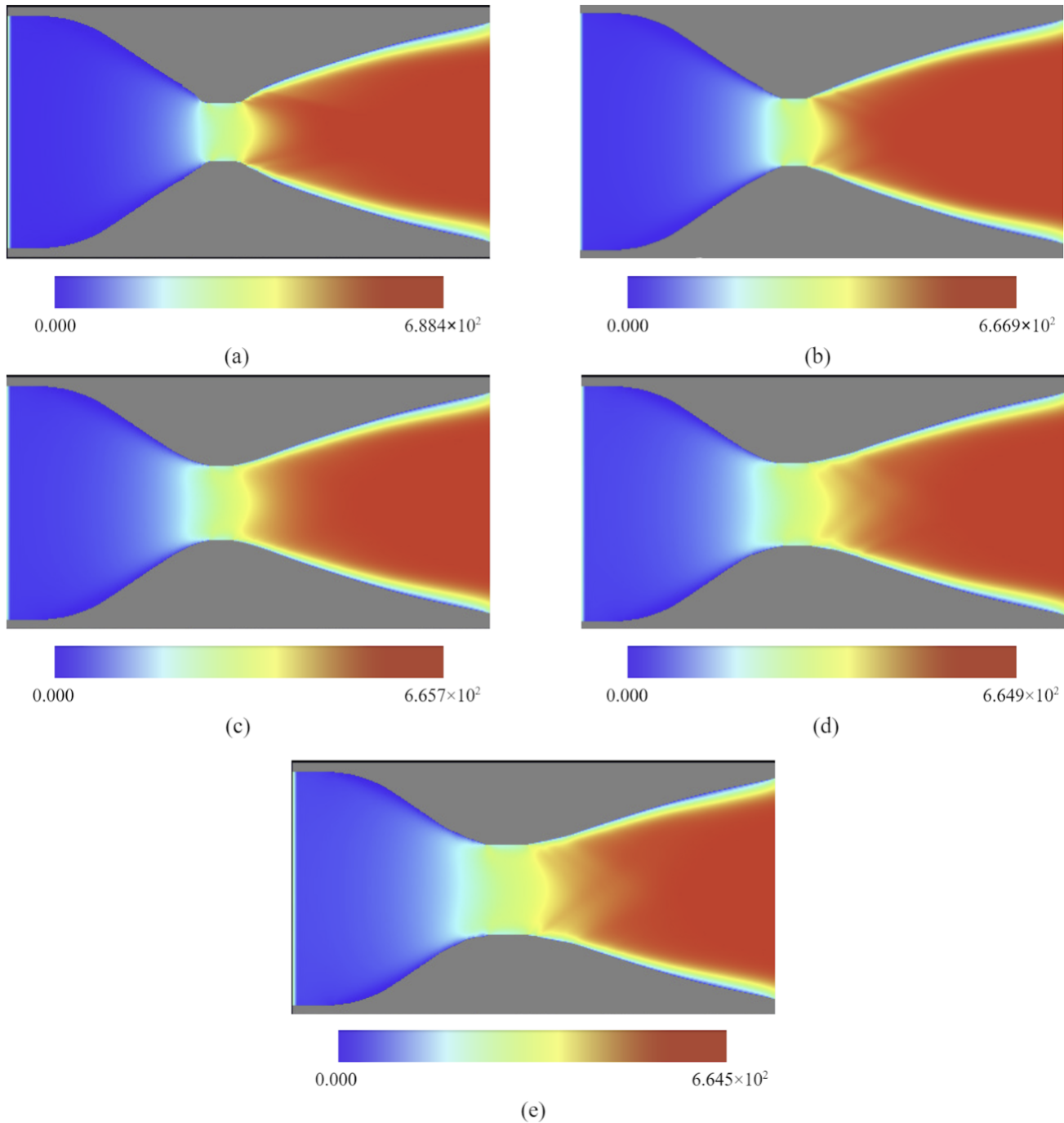
Figure 3 shows the fluid pressure of the flow through each of the five nozzles.. From Figure 3, it can see that the nozzles with a smaller throat diameter have a higher maximum fluid pressure (in the diverging section).

Figure 4 shows the fluid density of the flow through each of the five nozzles. Note that the simulation was run to a time of 8.0 ms (the flow was observed to be steady at this time). From Figure 4, it can see that the nozzles with a smaller throat diameter have a higher maximum fluid density (in the diverging section).

Figure 5 shows the temperature of the fluid of the flow through each of the five nozzles. Note that the simulation was run to a time of 8.0 ms (the flow was observed to be steady at this time). From Figure 5, it can see that the nozzles with a smaller throat diameter have a higher maximum fluid temperature (in the diverging section).

## Discussion

Table 1 shows the minimum and maximum fluid speed in the simulation domain for each nozzle studied. As seen from table 1,



**Fig. 2 .** Speed (velocity magnitude) for flow through each nozzle. (a) Nozzle A; (b) Nozzle B; (c) Nozzle C; (d) Nozzle D; (e) Nozzle E. Note that the color bar is scaled differently for each nozzle.

generally the maximum speed decreases with increase in throat diameter.

It is observed as the throat diameter increases down the column the minimum and maximum velocity decreases.

It is clearly observed that as the throat diameter of the nozzle increases the difference in pressure between the inlet and outlet of the nozzle decreases implying inverse proportionality.

The thrust force or the horizontal force depends on the throat

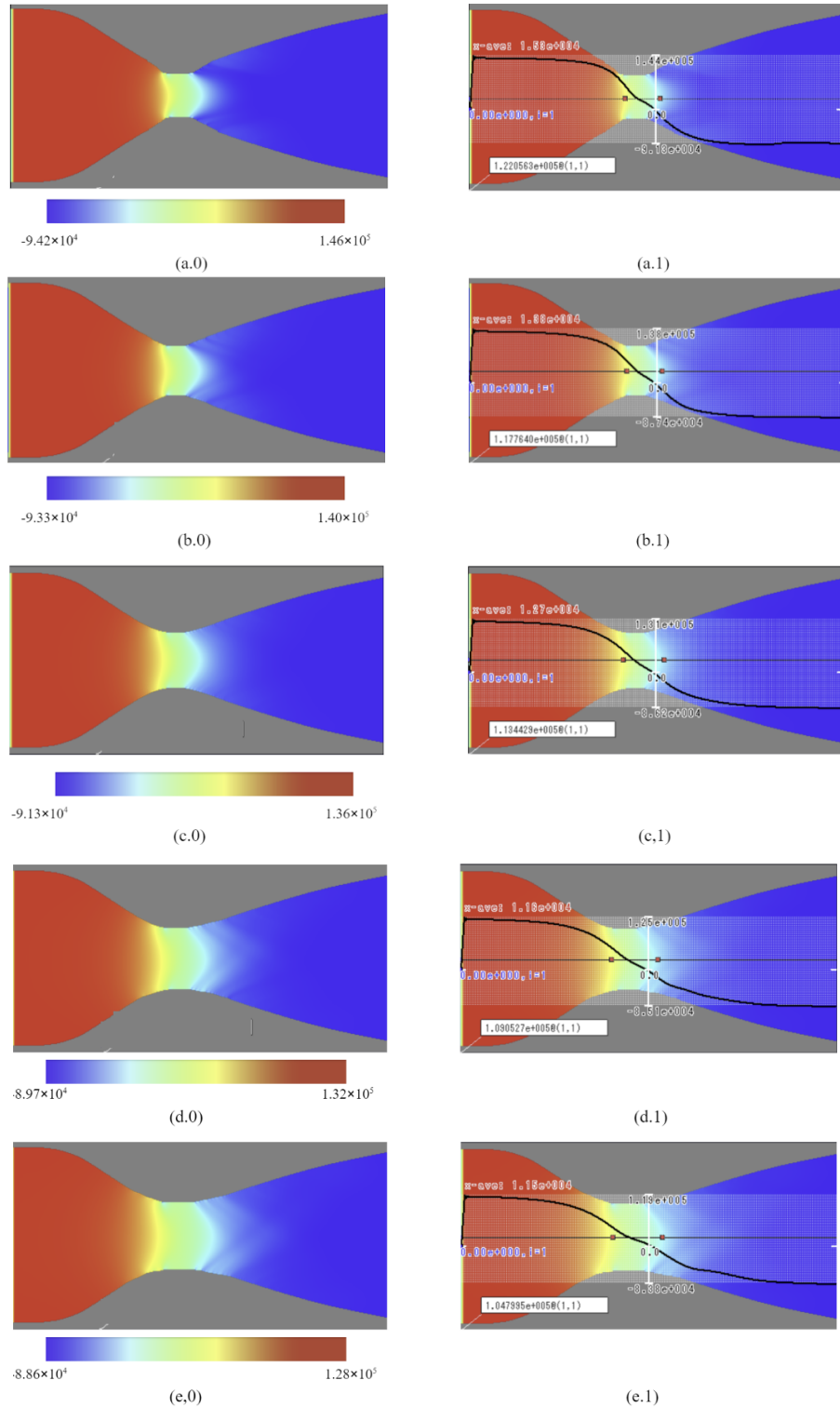


**Fig. 3** Pressure of flow through each nozzle. (a) Nozzle A; (b) Nozzle B; (c) Nozzle C; (d) Nozzle D; (e) Nozzle E. Note that the color bar is scaled differently for each nozzle.

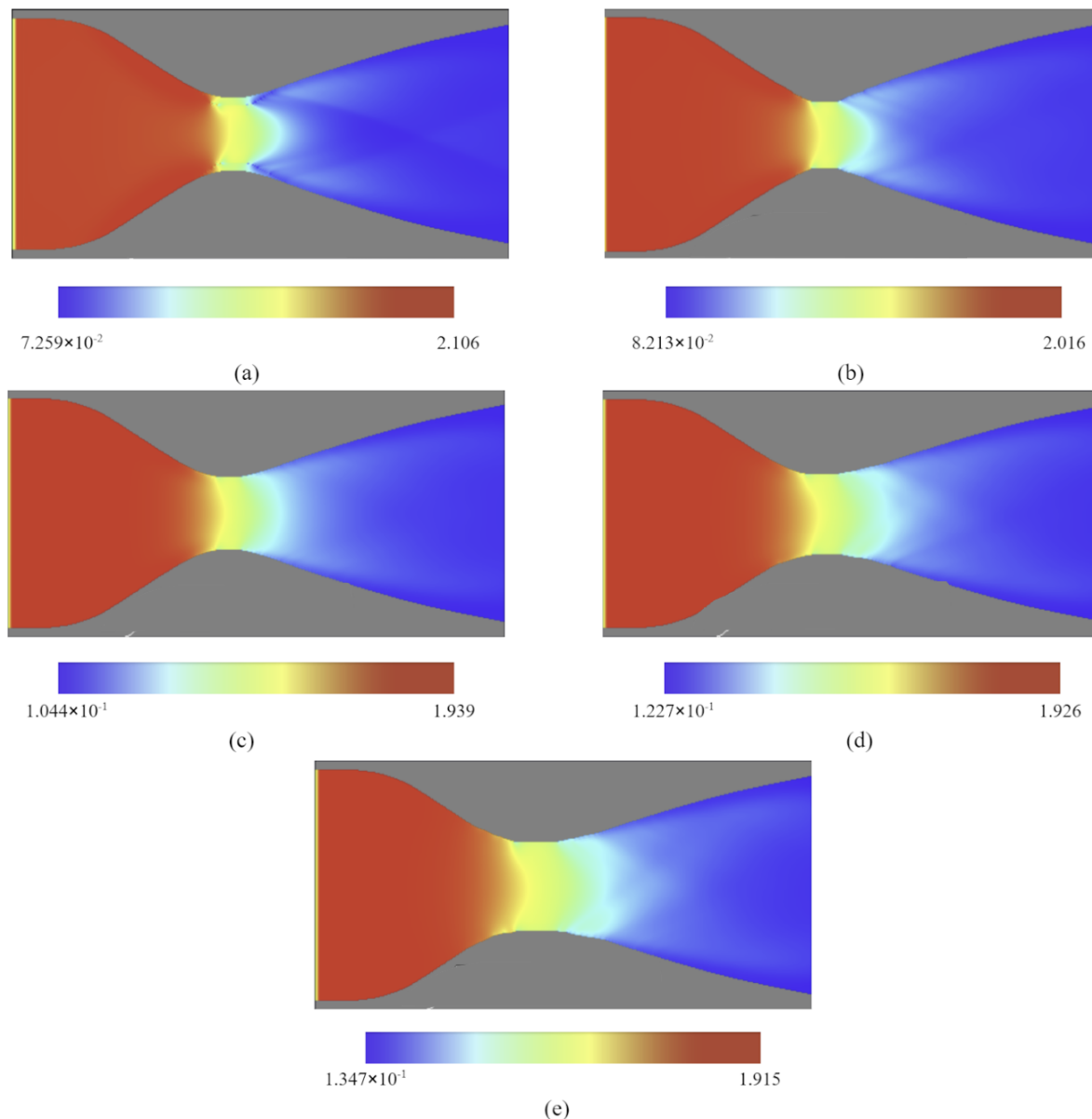


**Fig. 4** Density of fluid flowing through each nozzle. (a) Nozzle A; (b) Nozzle B; (c) Nozzle C; (d) Nozzle D; (e) Nozzle E. Note that the color bar is scaled differently for each nozzle.

diameter of the De Laval Nozzle. The variation of this thrust with respect to variation in throat diameter is given in Figure 7.

It is clearly observed that as the throat diameter of the nozzle increases the difference in pressure decreases implying inverse proportionality between them. Error bars can also be seen in the graph. These capture the geometric uncertainties of the nozzle geometries like symmetry and abnormal pixel placement.

To further investigate the physics of these flows, a simple 1D isentropic analysis was conducted. Assuming isentropic flow, Equation 1 was used to predict the nozzle exit velocity for

each nozzle. The pressure drop was taken from the Flowsquare simulation outputs. The results from these calculations, as well as the exit velocity results from Flowsquare, are shown in Figure 8. The values of the CFD analysis and theoretical analysis are similar<sup>1</sup>.

There is no significant difference in the value of nozzle parameters by the theoretical method, which uses formulae and CFD for the inviscid flow<sup>3</sup>.

For nozzle diameters greater than 88.3 mm, the CFD and isentropic flow results show excellent agreement. For smaller

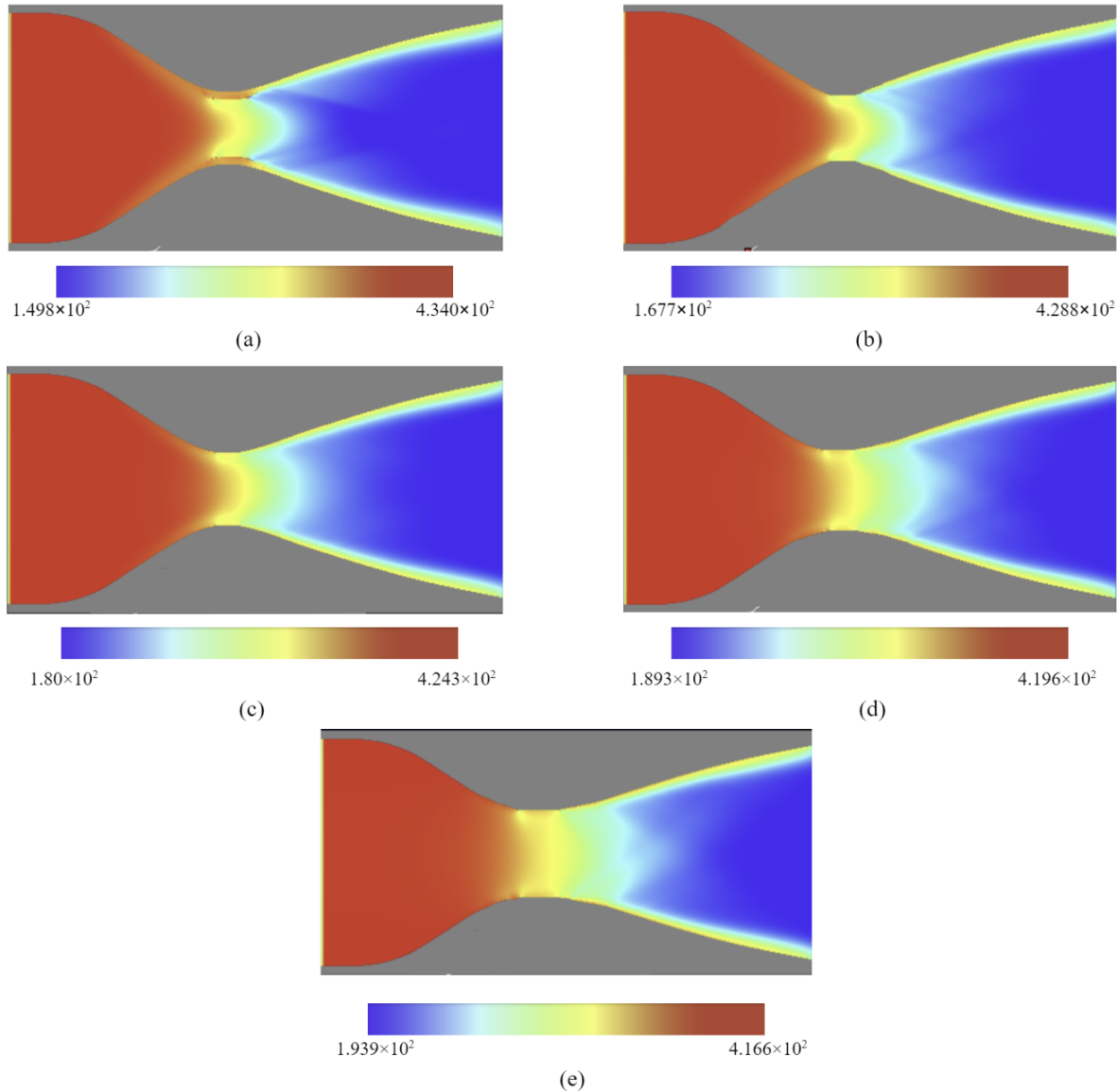


**Fig. 5** Temperature of fluid flowing through each nozzle. (a) Nozzle A; (b) Nozzle B; (c) Nozzle C; (d) Nozzle D; (e) Nozzle E. Note that the color bar is scaled differently for each nozzle.

nozzles, the isentropic model overpredicts the exit velocity as determined from CFD. This is likely because due to the narrow constriction in the small nozzle, the flow is more irreversible in nature, and thus deviates more strongly from isentropic.

## Conclusion

The results of this experiment indicate a clear relationship between the throat diameter of a De Laval nozzle and its performance characteristics, specifically thrust and gas exit velocity. Preliminary findings demonstrate that both thrust and gas exit

velocity increase as the throat diameter decreases. This relationship underscores the critical importance of precise throat design in optimizing nozzle performance. The implications of this study are significant for the fields of aerospace and propulsion engineering. The ability to fine-tune thrust and gas exit velocity through careful control of throat diameter offers a valuable tool for improving the efficiency and effectiveness of rocket and jet engines. Future research should focus on detailed flow analysis using computational fluid dynamics (CFD) simulations, as well as experimental validation under varying conditions to confirm the consistency of these findings. Additionally, exploring the impact of different materials, throat geometries, and propellant

Throat Diameter (mm)	Minimum Speed (m/s)	Maximum Speed (m/s)
69.6	344.2	688.4
79.0	346.9	669.7
88.3	334.8	665.7
97.7	332.4	664.9
107.1	327.3	654.5

**Table 1** Minimum and maximum fluid speed for each nozzle studied.

Throat Diameter [mm]	Predicted Exit Velocity [m/s]	CFD Exit Velocity [m/s]	Percent Discrepancy [%]
69.6	704	663	6.2
79.0	688	661	4.1
88.3	667	669	-0.3
97.7	664	664	0.0
107.1	648	653	-0.7

**Table 2** Comparison of predicted exit velocity and experimental velocity

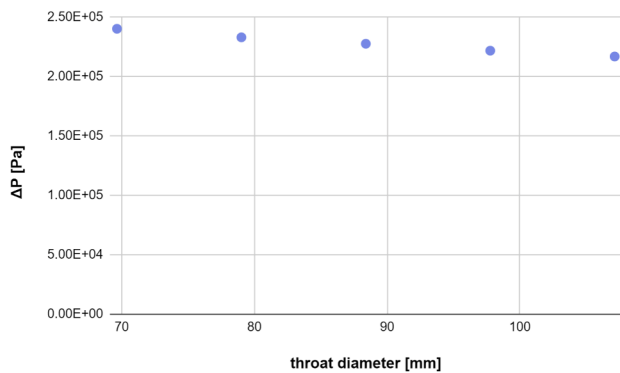


**Fig. 6** Graph of variation of  $\Delta P$  against variation in throat diameter

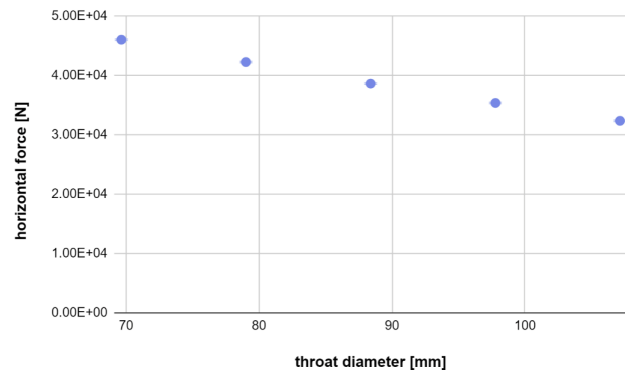


**Fig. 7** Graph of variation of Thrust against variation in throat diameter

types will further refine our understanding and application of these principles. In conclusion, the study provides insights into the design and optimization of De Laval nozzles, paving the way for enhanced propulsion systems. By continuing to explore and refine these principles, significant advancements in propulsion technology, contributing to more efficient and powerful aerospace applications, can be achieved.

## Acknowledgements

Thank you for the guidance of Scott Elgersma from Lumiere Foundation in the development of this research paper.

## References

- 1 M. Patel, *Concepts and CFD analysis of de-Laval nozzle*.
- 2 N. Deshpande and S. Vidwans, *Theoretical and CFD Analysis of De Laval Nozzle*.
- 3 Kamal Gautam, *Dynamics and Thrust Generation in De Laval Nozzles: A Study Using ANSYS Fluent*.
- 4 *Analysis of De Laval Nozzle Geometry Effect of Gas Pressure Variation at the Entrance*.